A parametric study of methanol crossover in a flowing electrolyte-direct methanol fuel cell

E. Kjeang [a], J. Goldak [b], M.R. Golriz [a,*], J. Gu [b], D. James [c], K. Kordesch [d]

[a] Department of Applied Physics and Electronics, Umeå University, Umeå SE-90187, Sweden
[b] Department of Mechanical and Aerospace Engineering, Carleton University, 1125 Colonel By Dr., Ottawa, Ont., Canada K1S5B6
[c] Fuel Cell Division, Energy Visions Inc., 3608 33rd St. NW, Calgary, Alta., Canada T2L2A6
[d] Technical University Graz, Institute for Inorganic Technology, Stremayrgasse 16/III, A-8010 Graz, Austria

Abstract

Direct methanol fuel cells (DMFCs) have significant potential to become a leading technology for energy conversion in a variety of applications. However, problems, such as methanol crossover reduce the efficiency and open circuit voltage of the cells. The novel design of flowing electrolyte-direct methanol fuel cells (FE-DMFCs) addresses this issue. Methanol molecules are effectively removed from the membrane electrode assembly (MEA) by the flowing electrolyte, and the unused fuel can be utilized externally.

In this paper, a general 3D numerical computational fluid dynamics (CFD) model is established to simulate methanol crossover by convection–diffusion in the FE-DMFC. Illustrations of methanol concentration distribution and methanol molar flux densities are presented, and the performance is compared to conventional DMFCs. The results indicate that methanol crossover can be reduced significantly. A parameter study is performed where the influences of anode fuel feed concentration, electrolyte channel thickness and electrolyte volumetric flow rate on methanol crossover are evaluated. In addition, effects of various electrolyte channel orientations are determined. According to the simulations, counter flow is the superior choice of channel orientations to minimize crossover.
© 2005 Elsevier B.V. All rights reserved.

Keywords: Direct methanol fuel cell (DMFC); Methanol crossover; Numerical modeling; Simulation; Flowing electrolyte; Proton exchange membrane (PEM)

1. Introduction

The research efforts and interests in fuel cell technology and development are increasing rapidly. Governments, companies and universities worldwide are gradually adapting to this new technology. Due to high efficiency and low emissions, fuel cells display a great variety of potential applications. The absence of moving parts and an extremely simple mechanism make fuel cells very competitive for small-scale applications. For such applications, low-temperature fuel cells with proton exchange membranes (PEM) are being adopted. Currently, efficient hydrogen PEM fuel cells dominate the market, but the problems with hydrogen storage and distribution are severe. Liquid fuels are much easier to handle although the conversion in fuel cells is more complex. One of the best available liquid fuels in terms of system overall efficiency (also called well to wheel efficiency) is methanol [1] that can be utilized directly in a direct methanol fuel cell (DMFC). However, the DMFC cannot yet compete with hydrogen fuel cells for transportation purposes, mostly due to its comparatively low cell efficiency and expensive catalysts [2]. On the other hand, for systems where size and weight are more important, it exhibits high potential. The power densities and energy densities of DMFCs are superior, even when compared to newly developed lithium ion batteries [2]. The current obstacles are low cell efficiency and high cost, factors that must be improved to enable commercialization.

The efficiency of direct methanol fuel cells is reduced by two main bottlenecks, slow anode reaction kinetics and methanol crossover. Methanol crossover can be particularly severe in DMFCs with polymer electrolytes. Investigations

---

* Corresponding author. Tel.: +46 90 786 7431; fax: +46 90 786 6469.
E-mail address: mohammad.golriz@tfe.umu.se (M.R. Golriz).

Nomenclature

A	area (m^2)
c	concentration of methanol ($mol\,m^{-3}$)
c_v	specific heat at constant volume ($J\,kg^{-1}\,K^{-1}$)
c_2	concentration of methanol at the cathode side of the PEM ($mol\,m^{-3}$)
D	solute diffusivity ($m^2\,s^{-1}$)
ΔE	activation energy ($J\,mol^{-1}$)
Fo	Fourier number
i	cell current density ($A\,m^{-2}$)
k_1	constant of linearity
k_c	constant
k_p	constant
k_i	constant
K	constant related to effective hydraulic permeability ($m^2\,s^{-1}\,atm^{-1}$)
L_{PEM}	thickness of membrane (m)
L_x	length of MEA in FE flow direction (m)
L_y	thickness of FE channel (m)
L_z	width of MEA transverse to FE flow direction (m)
$\dot{n}$	methanol molar flux density ($mol\,s^{-1}\,m^{-2}$)
P	pressure (atm)
$\dot{q}$	internal heat source ($W\,m^{-3}$)
R	universal gas constant ($J\,mol^{-1}\,K^{-1}$)
S	source of species ($mol\,s^{-1}$)
t	time (s)
T	temperature (K)
v	fluid velocity ($m\,s^{-1}$)
$\dot{V}$	volumetric flow rate ($m^3\,s^{-1}$)
x	direction of FE flow
y	direction across FE channel
z	direction of FE channel width

Greek letters

α	thermal diffusivity ($m^2\,s^{-1}$)
κ	thermal conductivity ($W\,m^{-1}\,K^{-1}$)
λ	coefficient of electro-osmosis (number of methanol molecules dragged by each proton)
μ	chemical potential ($J\,mol^{-1}$)
μ_v	kinematic viscosity ($kg\,m^{-1}\,s^{-1}$)
ρ	density ($kg\,m^{-3}$)

Subscripts

a	anode
ave	average value
c	cathode
FE	flowing electrolyte
max	maximum value
PEM	proton exchange membrane

of the most common solid polymer electrolyte material, Nafion®, have identified that methanol can penetrate sulfonic acid membranes [3]. It has also been shown that methanol crossover leads to a significant loss in oxygen reduction performance at the cathode due to a mixed potential. Apart from that, crossover is a substantial loss of fuel that produces no current whatsoever. Therefore, overall cell potential as well as fuel efficiency is limited by this effect. Control of anode fuel feed concentration And flow rate as well as utilization of effective methanol oxidizing anode catalysts are important strategies to minimize methanol crossover. There is much ongoing work in this field, and several more advanced methods of reducing crossover have been presented. For instance, the electrolyte material can be replaced [4,5] or be modified chemically [6,7] to achieve lower methanol permeation. Shim et al. [8] suggest the use of a methanol impermeable barrier between the electrodes, allowing protons to pass but preventing methanol molecules from reaching the cathode catalyst layer. A method has already been introduced based on a membrane electrode assembly concept invented by Kordesch et al. [9,10] where the membrane is replaced by a flowing electrolyte. This novel design efficiently removes methanol from the electrolyte department by simple convection. The methanol in the electrolyte can be separated e.g., by membrane methods and consumed or a small amount may be used up in a loaded control sensing cell which then automatically adjusts the methanol feed to the system [10]. Many numerical as well as mathematical models of the conventional DMFC can be found in the literature [11,12], but to make the FE-DMFC competitive much more work is needed. A mathematical model of the FE-DMFC has been developed by Golriz et al. [13], which can be extended by support of numerical simulations.

The objective of this paper is to model the electrolyte channel of a flowing electrolyte DMFC and numerically simulate the effect of methanol crossover for different operating conditions. Parameters, such as electrolyte flow rate, electrolyte channel thickness, fuel concentration and channel orientation will be studied in detail. Simulations of the conventional PEM-DMFC will also be performed and compared to the results of the FE-DMFC study. The model is intended to improve the knowledge of flowing electrolyte fuel cell performance and to serve as a vital part of a future optimization study.

2. Flowing electrolyte-direct methanol fuel cells

A general direct methanol fuel cell basically consists of a membrane electrode assembly (MEA) supported by gas diffusion layers and bipolar plates. The MEA contains two porous electrodes (anode and cathode) immersed in a proton-conducting electrolyte. Fuel (aqueous methanol) is supplied to the anode compartment and oxidizes at the catalyst layer to form carbon dioxide, protons and electrons. The protons diffuse through the electrolyte to the cathode compartment,
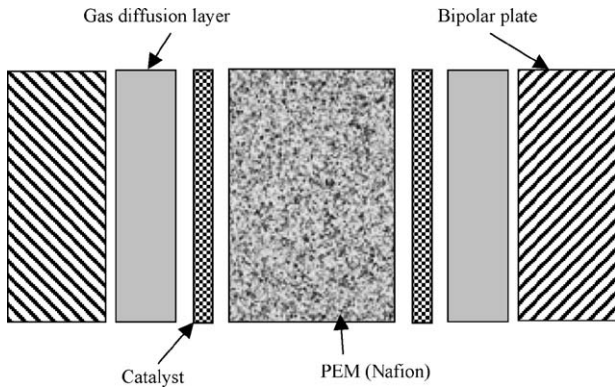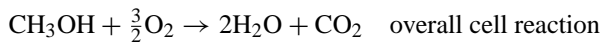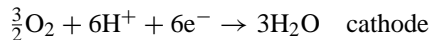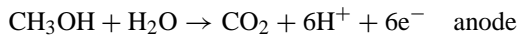
Fig. 1. 2D cut plane of a typical DMFC module with proton exchange membrane.

where they react with oxygen to produce water as the end product. The cell reactions are:

$$CH_3OH + H_2O \rightarrow CO_2 + 6H^+ + 6e^- \quad \text{anode}$$

$$\tfrac{3}{2}O_2 + 6H^+ + 6e^- \rightarrow 3H_2O \quad \text{cathode}$$

$$CH_3OH + \tfrac{3}{2}O_2 \rightarrow 2H_2O + CO_2 \quad \text{overall cell reaction}$$

The electrons generated at the anode flow through an external load before arriving at the cathode, thus providing useful electrical power. A schematic of a general DMFC with proton exchange membrane is presented in Fig. 1. The function of the membrane is to physically separate the electrodes, transfer protons from anode to cathode and act as an insulator to electric current. A good electrolyte shall have high proton conductivity, low methanol permeation and low electronic conductivity, and shall also be as thin as possible. Nafion® is the commonly used material, and very thin films can be produced. However, the problem of methanol permeation in these membranes leads to reduced cell voltage and low efficiency. The new concept of flowing electrolyte-direct methanol fuel cells (FE-DMFCs) addresses this issue. Here, in one configuration, an electrolyte channel is immersed between two thin 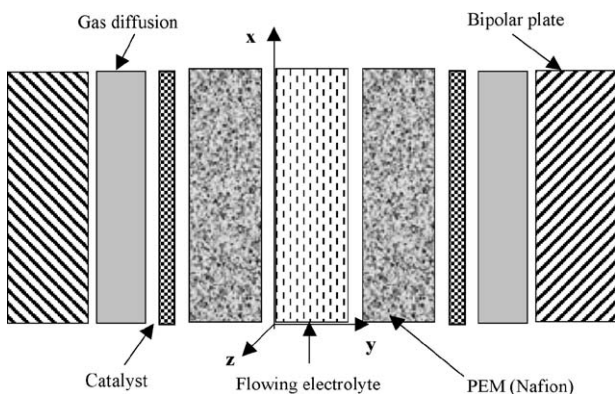PEM layers as in Fig. 2. The flowing electrolyte (dilute sulfuric acid) effectively removes methanol from the MEA by convection, and hinders its arrival at the cathode. The MEA of the second generation FE-DMFC, with a 50 mm × 50 mm surface area, still contains two thin layers of PEM (50 μm thick) attached to the electrodes. However, the main function of these layers is to physically separate the different channels of the cell. The PEM-layers could be considered optional and may be removed or replaced by a thinner and cheaper material. The electrolyte channel width is a target for optimization. Other advantages of a circulating electrolyte system are simple thermal and water management; the possibility to remove side reaction products and impurities, such as aldehyde residues, carboxylic acids or other intermediates produced during the oxidation of methanol; and the option to adjust the electrolyte flow rate relative to current density or fuel concentration to minimize fuel crossover. Moreover, methanol transport from the fuel channel to the anode catalyst layer is enhanced by the flowing electrolyte, which has been shown to improve performance at high current densities [14]. The flowing electrolyte configuration does however add some extra complexity to the system, e.g., electrolyte piping and pump.

3. Method

As mentioned in the introduction, the objective of this work is to create a numerical model of the electrolyte compartment of the FE-DMFC and to simulate methanol crossover for various operating conditions. All parts of the fuel cell MEA between the catalyst layer of the anode and the catalyst layer of the cathode are included in the domain. The catalyst layers of the electrodes are assumed to be infinitely thin. The structure of the electrolyte department in a FE-DMFC is displayed in Fig. 2. Notice that it consists of two proton exchange membranes with a flowing electrolyte channel in between. A three-dimensional model is necessary due to the geometry of the fuel cell in general and the electrolyte channel fluid flow in particular. For this purpose, a computational fluid dynamics (CFD) model is an obvious choice.

Methanol crossover in direct methanol fuel cells occurs due to the driving forces of chemical potential gradients, pressure gradients and electro-osmosis [15]. For solutes, the chemical potential gradient equals the concentration gradient. If the solute diffusivity is assumed to be independent of concentration, the steady state methanol molar flux density across the membrane of a PEM-DMFC is described by

$$
\begin{aligned}
\dot{n}_{\text{MeOH}} &= -\frac{D}{L_{\text{PEM}}}\Delta c - \frac{c_2 K}{L_{\text{PEM}}}\Delta P + \frac{\lambda}{nF}i \\
&= k_c \,\Delta c + k_p \,\Delta P + k_i i
\end{aligned}
\tag{1}
$$

According to the model of a conventional DMFC presented by Wang and Wang [12], the flux due to the pressure gradient in this equation is small compared to the other fluxes

Fig. 2. 2D cut plane of the corresponding FE-DMFC with flowing electrolyte (simplified geometry, not to scale).

and can therefore be neglected. At low current densities, the diffusion flux dominates and electro-osmosis flux is small. However, at high current densities both fluxes are significant. In a FE-DMFC, with a fluid flow present and an Eulerian formulation, diffusion is replaced by convection–diffusion. The process is more complex than pure diffusion, but the dominant effect is a suction mechanism that enhances mass transfer by convection–diffusion through the anode side membrane. The electro-osmotic contribution, on the other hand, does not change when the flowing electrolyte convection effect is introduced. In this context, especially if we restrict the operating range to the low current density regime, the contribution of electro-osmosis may also be neglected. The flux in the membrane is thus simplified to

$$\dot{n}_{MeOH} = -\frac{D}{L_{PEM}}\Delta c \qquad (2)$$

In this paper, only the convection–diffusion contribution is being analyzed. The diffusivity then becomes a crucial parameter for the quality of the results.

For the FE-DMFC, the temperature dependence of the diffusivity of methanol in Nafion®, $D_{MeOH/PEM}$, as well as methanol in water, D_{MeOH/H_2O}, must be determined (except for its high proton conductivity, dilute sulfuric acid is assumed to have the same properties as water). In general, diffusivity exhibits exponential temperature dependence, such as

$$D(T) = D_{ref} \exp\left(\frac{\Delta E}{R}\left[\frac{1}{T_{ref}} - \frac{1}{T}\right]\right) \qquad (3)$$

Scott et al. [16] suggest $D_{MeOH/PEM} = 4.9 \times 10^{-10}\,m^2\,s^{-1}$ at 333 K and $D_{MeOH/H_2O} = 2.8 \times 10^{-9}\,m^2\,s^{-1}$ at 363 K as reference values for the relationship in Eq. (3), and $\Delta E/R = 2436\,K$ for Nafion® 117. However, several other functions can be found. Kulikovsky [17] recommends the reference value of methanol diffusivity in water in void pores to be $D_{ref} = 1.58\,10^{-9}\,m^2\,s^{-1}$ at $T_{ref} = 298\,K$, and use the temperature dependence

$$D_{MeOH/H_2O}(T) = D_{ref} \exp(0.026236(T - T_{ref})) \qquad (4)$$

This is in agreement with the reference value for methanol in water given by Physics Handbook [18], $D_{MeOH/H_2O} = 1.4 \times 10^{-9}\,m^2\,s^{-1}$ at 291 K, although both differs significantly from the value used by Scott et al. [16]. For methanol in Nafion®, Kulikovsky [17] uses

$$D_{MeOH/PEM}(T) = 4.012 \times 10^{-13} \exp(0.024312T) \qquad (5)$$

This function is also different than the function given by Scott et al. [16]. For this work, the diffusivities given by Scott et al. [16] are chosen, mainly because the operating temperature of the FE-DMFC is in the same range as their reference values. Note that the uncertainty of these values can be considered high.

The steady-state velocity profile in the FE channel is calculated based on conservation of mass and momentum in three dimensions. Conservation of mass for incompressible fluids can be described by the 3D continuity equation

$$\nabla \cdot \bar{v} = 0 \qquad (6)$$

No-slip boundary conditions and the Reynolds number flow imply that $v_y = 0$ and $v_z = 0$ in the entire channel. Thus, assuming that the flux of methanol and water across the anode side membrane is small compared to the electrolyte flow, fluid flow takes place in the x-direction only. Momentum conservation is described by the 3D Navier–Stokes equation for incompressible fluids

$$\rho\frac{\partial\bar{v}}{\partial t} + \rho\,(\bar{v}\cdot\nabla)\,\bar{v} = -\nabla P + \rho\bar{g} + \mu_v\,\nabla^2\bar{v} \qquad (7)$$

If gravity is ignored, the steady-state equation can be written as

$$\rho(\bar{v}\cdot\nabla)\bar{v} = -\nabla P + \mu_v\,\nabla^2\bar{v} \qquad (8)$$

For the particular geometry of the FE channel (main flow in x-direction from inlet to outlet, channel width much larger left to right (z) than between the top and bottom membranes (y)) the flow in the middle of the channel can be modeled as a two-dimensional steady-state flow between two plates caused by a pressure gradient in the x-direction (Poiseuille flow). The solution of Eq. (8) with no-slip boundary conditions is a linear pressure gradient, Π, along the electrolyte flow direction, and

$$v_x(y) = \frac{\Pi}{2\mu_v}y\,(L_y - y) \qquad (9)$$

This fully developed parabolic velocity profile has zero velocities at the top and bottom membrane surfaces and a maximum in the center of the channel. It is assumed to be representative for the bulk of the flow, except near the left and right channel edges at $z = 0$ and L_z. The thickness of these edge effects is assumed to be of the same order of magnitude as the channel thickness between the membranes. The velocity profile is assumed to have a parabolic shape where edge effects are present, with zero velocity at the edge increasing gradually to the free stream velocity as one moves away from the edge. The free stream velocity is determined by Eq. (9) independently of the z-coordinate. The volumetric flow rate and mean velocity are obtained by surface integration. The Reynolds number is calculated by

$$Re = \frac{\rho v_{max}L}{\mu_v} \qquad (10)$$

The characteristic length of the FE channel is its thickness, L_y. Reynolds numbers are in the range $0.5 \le Re \le 10$, thus indicating laminar flow.

To solve the mass transfer problem in the presence of a velocity field, convection as well as diffusion must be considered. Conservation of species gives the convection–diffusion equation for time dependent solute diffusion in 3D as

$$\frac{\partial\mu}{\partial t} + \bar{v}\cdot\nabla\mu + \nabla\,(-D\,\nabla\mu) = S \qquad (11)$$

For a dilute species in a liquid solvent, one can assume that the chemical potential equals solute concentration. Thus, with no internal chemical reactions or sources one finally obtains Fickian advection–diffusion

$$\frac{\partial c}{\partial t} + \bar{v} \cdot \nabla c + \nabla(-D \nabla c) = 0 \tag{12}$$

The time dependent solute convection–diffusion equation in the presence of a velocity field, Eq. (12), applied to the fuel cell MEA domain, is solved using an in-house CFD software called SimManTec Framework. In this software code, the solute convection–diffusion equation is solved using a 3D transient non-linear space–time method. The method treats time dependent problems like stationary problems using space–time meshes that discretize space and time independently. Usually, finite element methods use a semi-discrete algorithm, i.e., discretizes space using FEM and use what can be considered a finite difference method, such as Crank–Nicholson in time. In problems where the domain undergoes deformations in time, the classical finite difference approach may become difficult to use. The space–time domain can be considered a four dimensional continuum, where time is treated as the fourth dimension space variable. But since information is transferred from earlier to later times, the standard stepwise approach from finite differences is preserved. A continuous Galerkin method in space and a discontinuous method in time are used for the discretization.

The methanol crossover model of the FE-DMFC is incorporated as a time dependent problem with constant velocity. Time step size is chosen according to the accuracy criterion $0.1 < Fo < 10$, based on the dimensionless Fourier number

$$Fo = \frac{D \, \Delta t}{\Delta y^2} \tag{13}$$

For the solute convection–diffusion problem, Δ_y represents the mesh element size in the anode-to-cathode direction across the FE channel. The operating temperature is set to 60 °C. Dirichlet boundary conditions are applied to the anode and cathode surfaces facing the membranes. Either constant or linear methanol concentration in the range of 1–4 M is applied at the anode surface, and zero concentration at the cathode surface. Note that the anode surface concentration is expected to be somewhat lower than the fuel feed concentration, due to the concentration drop across the fuel diffusion layer. Also, zero concentration at the cathode indicates that all methanol molecules reaching the cathode surface are being oxidized instantly at the catalyst sites. Neumann boundary conditions with zero molar flux density are applied to all other surfaces.

4. Results and discussion

4.1. Mesh convergence analysis and model validation

To get accurate results using the convection–diffusion solver it appears to be crucial to employ elements that are not too distorted or elongated. If the aspect ratio of the element blocks becomes too large, the solution may not converge. For the geometry of the MEA, which has thin membrane films of aspect ratios up to 1000, this is particularly important. When meshing the MEA, this implies that the number of elements becomes very large. For accuracy purposes on one hand and computational time on the other, a good compromise is found with eight elements of eight-node bricks across the electrolyte channel. The error using this mesh is expected to be less than 0.2% compared to an ideal mesh.

The model is validated for the case with zero FE velocity, which is a straightforward analytical calculation using Eq. (12). With zero velocity, the steady-state solution is

$$\dot{n} = -D \nabla c = -D \frac{\Delta c}{L_y} \tag{14}$$

This constant methanol molar flux implies a linear concentration distribution across the membranes and the stationary electrolyte. The gradient is higher in the membrane material (low diffusivity) than in the flowing electrolyte (high diffusivity) and

$$c_a - c_c = \Delta c_{PEM} + \Delta c_{FE} \tag{15}$$

In this equation, Δc_{PEM} represents the sum of the concentration drops across both membranes in the MEA of the FE-DMFC. A simulation of the model is run for a single slice in the z-direction. The development of the expected concentration profile with time is monitored and steady-state is verified. Total methanol molar flux is determined by post-processing surface integration applied to the membrane parts. The average molar flux across the anode side PEM membrane is computed by

$$\dot{n}_{ave} = \frac{1}{A_{PEM}} \int \int_A \dot{n} \, dA \tag{16}$$

This gives $\dot{n}_{ave} = 0.00671 \, mol \, s^{-1} \, m^{-2}$, which is constant throughout all parts when the electrolyte is immobile. The deviation from the analytical result is 0.03%. Also, the resulting concentration distribution is clearly linear as expected.

4.2. 3D simulations

As a result of the mesh convergence analysis, 3D simulations of the entire domain from anode to cathode with cubic elements become computationally expensive. A symmetry plane in the middle of the FE channel ($z = 25$ mm) is identified, cutting the MEA into two equivalent parts in order to reduce the number of elements. Complete 3D simulations demand a trade-off in accuracy but for illustrative purposes the precision is still acceptable.

Methanol crossover 3D simulations of the MEA part of the FE-DMFC is performed for the case with electrolyte flow rate $\dot{V} = 0.02 \, cm^3 \, s^{-1}$, FE channel thickness $L_y = 0.6$ mm and constant anode concentration $c_a = 4$ M. The time step size is chosen to have a Fourier number in the range $0.1 < Fo < 10$,

and a time dependent simulation is run until steady state is reached. Element Courant numbers are determined by

$$Co = \frac{v_{\max}\,\Delta t}{\Delta x} \qquad (17)$$

For the time step size chosen, $Co = 20$. The physical ratio of convection to diffusion is determined by the Peclet number for the problem

$$Pe = \frac{L_x v_{\text{ave}}}{D} = 3 \times 10^4 \qquad (18)$$

Apparently, convection is much stronger than diffusion. The results obtained consist of a velocity profile, methanol concentration distribution and molar flux density at all nodes. As described, the velocity has a fully developed parabolic Poiseuille profile across the thickness of the FE channel. In the z-direction, the bulk of the flow is uniform except near the edges, where it is parabolic due to edge effects. For this velocity profile, the volumetric flow rate must be determined by surface integration applied to the channel intersection

$$\dot{V} = \int \int_A v_x\,\mathrm{d}A \qquad (19)$$

The total volumetric flow rate becomes $\dot{V} = 1.81 \times 10^{-8}\,\mathrm{m^3\,s^{-1}}$, which is slightly lower than for the single slice model because of the edge effects in z. Edge effects can also be seen in the concentration distribution. Near the very edge, where the velocity approaches zero, the concentration is linear across the FE channel. This is not the case in the bulk of the fluid flow, where the flowing electrolyte efficiently removes most of the methanol penetrating the anode side membrane. A contour plot of methanol concentration in the middle of the FE channel is presented in Fig. 3. The figure clearly shows the build-up of a concentration edge effect in the z-direction, which appears to have the same thickness as for the velocity. The contours indicate that the bulk of the flow has uniform concentration distribution along the z-axis. In the case with zero fluid velocity, the concentration in the bulk would be equal to the concentration at the edge (pure diffusion). Obvi-
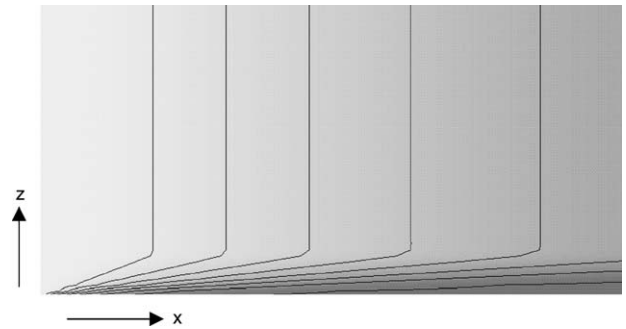

Fig. 3. Methanol concentration (shaded) in the center of the FE channel ($L_y = 0.3$ mm). Fluid flow is in the x-direction. The contours represent constant concentration.

ously, convection is the dominate means of mass transfer in the electrolyte channel.

Methanol molar flux density across the anode and cathode surfaces is shown in Fig. 4. Methanol crossover (cathode flux) is significantly higher near the outlet of the channel than close to the inlet. On the other hand, molar flux across the anode has its maximum at the channel inlet, and decreases along the flow direction. At the edge ($z = 0$), the flux across the anode is the same as the flux across the cathode (except near the inlet). That means, where the fluid velocity is zero no species are removed by convection and the only transport mechanism is pure diffusion. Further away from the edge, convection dominates. At a short distance from the edge, the flux is approximately the same as in the middle of the channel ($z = 25$ mm). Note that the anode flux is significantly larger than for pure diffusion due to the suction effect at the anode surface. The suction effect may enhance mass transfer in the catalyst layer of the anode and improve reaction-rates and efficiency. Contrarily, more methanol will mix into the flowing electrolyte. It is thus necessary to process or consume this electrolyte and methanol mixture externally. However, it is even more important to keep methanol away from the cathode catalyst layer. For this purpose, the flowing electrolyte shows great promise. Except very near the z-edge where the velocity
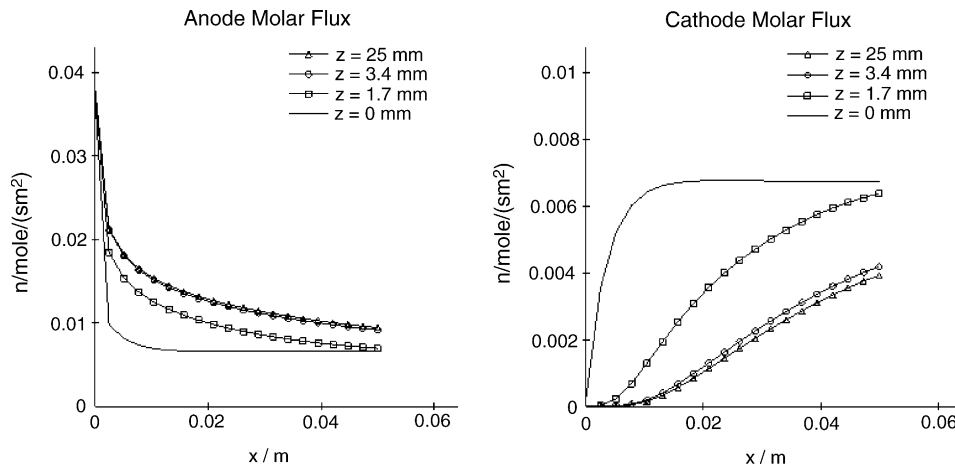

Fig. 4. Anode (a) and cathode (b) methanol molar flux density along the direction of fluid flow (x) for various distances from the edge (z).

is too small, methanol crossover is reduced to a minimum. The average molar flux density across anode and cathode is calculated by surface integration as in Eq. (17) to $\dot{n}_a = 0.01284 \, \mathrm{mol \, s^{-1} \, m^{-2}}$ and $\dot{n}_c = 0.001962 \, \mathrm{mol \, s^{-1} \, m^{-2}}$. In this case, 85% of the fuel penetrating the anode is removed by the flowing electrolyte, which is more than three times better than the case with zero electrolyte velocity.

As a comparison, this model is also run for the PEM-DMFC case, where the flowing electrolyte channel is removed completely. The two membranes are merged to one single membrane of thickness 0.1 mm. For this simple geometry, methanol flux is entirely one-dimensional and all of the species penetrating the anode will arrive at the cathode. The results for $c_a = 4 \, \mathrm{M}$ and $c_c = 0 \, \mathrm{M}$ are $\dot{n}_a = \dot{n}_c = 0.0196 \, \mathrm{mol \, s^{-1} \, m^{-2}}$. The methanol crossover in the FE-DMFC is reduced by 90% compared to this result.

4.3. Parameter study

For the overall performance of the FE-DMFC, a 3D model of at least half the MEA is essential. However, it is excessive for a detailed parameter study. A basically two-dimensional model of one single slice in the middle of the channel ($z = 25 \, \mathrm{mm}$), like the one used in the mesh convergence analysis, is instead considered. This slice with only one element in the z-direction is assumed to be representative for the whole geometry. From a system point of view, the edge effect should be included. However, since the bulk of the geometry dominates the performance of the electrolyte channel, the single slice model serves the purpose of a parameter study. Simulations on the single slice domain are carried out for a variety of parameter input data. Methanol crossover can be modeled as a function of several variables, such as operating temperature, pressure, FE velocity field and flow rate, FE channel dimensions, methanol concentration at anode and cathode, current density, cell voltage, etc. In this preliminary parameter study, focus is on three of these variables; methanol concentration at anode, electrolyte volumetric flow rate and FE channel thickness. The temperature is constant at $60\,^{\circ}\mathrm{C}$, the cathode concentration is assumed to be zero and the methanol flux density is assumed to be independent of the other variables. Thus,

$$\dot{n} = f(c_a, \dot{V}, L_y) \tag{20}$$

Since the concentration gradient is included in both time-independent terms in the convection–diffusion equation, Eq. (13), the anode concentration is expected to be an independent variable and is therefore treated separately, as in

$$\dot{n} = f(c_a) \cdot f(\dot{V}, L_y) \tag{21}$$

If the flow rate and channel thickness are held constant, one gets a linear concentration dependency
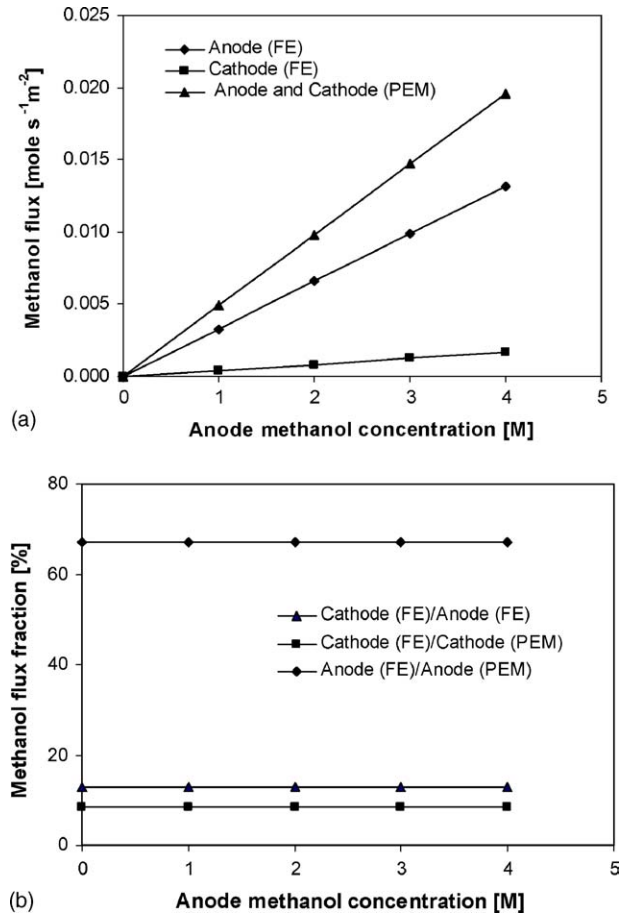
$$\dot{n} = k_1 \cdot c_a \tag{22}$$

Fig. 5. (a) Average methanol molar flux density across anode and cathode vs. anode surface concentration for FE-DMFC and PEM-DMFC. (b) Methanol molar flux density fractions. Conditions: volumetric flow rate $0.02 \, \mathrm{cm^3 \, s^{-1}}$ and channel thickness 0.6 mm.

Plots of the simulation outcome of methanol molar flux density across anode and cathode as a function of anode concentration are presented in Fig. 5a. Methanol crossover in the FE-DMFC equals cathode flux. Results for the PEM-DMFC are also shown, and for this type, methanol flux (crossover) is the same at both electrodes. Fig. 5b displays three different flux fractions; crossover fraction for FE-DMFC, crossover fraction compared to PEM-DMFC and anode flux fraction compared to PEM-DMFC. These plots clearly show that methanol molar flux is directly proportional to anode surface concentration, which confirms the dependency suggested in Eq. (22). The quantitative results are similar to the results of the complete 3D simulation: methanol flux across the cathode is 87.2% lower than the anode flux, and methanol crossover is reduced by 91.4% compared to the PEM-DMFC. The reductions obtained are independent of anode concentration. Additional tests are performed for other values of $\dot{V}$ and L_y, and these results also show a linear dependency.

The results obtained for $c_a = 4 \, \mathrm{M}$ are also used to evaluate the accuracy of the single slice model. Table 1 shows average values of methanol flux from the single slice model as well as the full 3D model, which is used as the reference case.

Table 1
Comparison of the results obtained with the single slice model and the full 3D model

|	Single slice model	Full 3D model	Diff. (%)
$\dot{n}_a$ (mol s^{-1} m^{-2})	0.01314	0.01284	+2.3
$\dot{n}_c$ (mol s^{-1} m^{-2})	0.001677	0.001962	−14.5
$\dot{V}$ (cm^3 s^{-1})	0.0197	0.0181	+8.8

As the single slice model ignores the edge effects at the left and right channel edges, it is expected to overestimate the reduction of methanol crossover. This is confirmed by the 14.5% reduction in flux across the cathode compared to the 3D case. In the same manner, anode flux is slightly higher. Moreover, the electrolyte flow rate is 8.8% higher than for the full 3D model that justifies the changes in methanol flux. Considering the fact that the models operate at different flow rates, the results of the single slice model are quite reasonable. In practice, edge effects can be avoided by constructing the electrolyte channel a few millimeters wider than the catalyst surfaces at the electrodes.

Simulations are run for several combinations of the two other variables, FE volumetric flow rate and FE channel thickness. Four different levels of each variable are used, and methanol concentration at the anode surface is constant. Element Courant numbers for the single slice model are in the range $5 < Co < 50$ and the problem Peclet numbers are between 10^4 and 10^5. The results of these tests are summarized in the surface plots in Fig. 6, which display the average methanol molar flux density as a function of both variables. The anode molar flux increases with flow rate and decreases with channel thickness. The methanol suction effect apparently is enhanced by an electrolyte high velocity and a thin channel. However, the appropriateness of inducing methanol suction is a matter for future consideration: it may be preferable to avoid methanol penetration of the anode, thus minimizing anode flux and the need for processing of unused fuel. For this scenario, a wide channel with a low flow rate is favorable. Nevertheless, anode flux in the FE-DMFC is still far below the value of the PEM-DMFC (0.02 mol s^{-1} m^{-2}). Cathode molar flux density (methanol crossover) on the other hand, is most certainly a means of minimization. Fig. 7 displays the achieved reduction of crossover compared to the equivalent PEM-DMFC. To reduce crossover, high FE flow rates and wide channels are to be used. The effect of increasing either one of them appears to be of the same magnitude. Notice that except for the cases with zero flow rates, the crossover reduction is more than 65% for all combinations being tested.

It is also obvious that the volumetric flow rate and channel thickness variables cannot be treated independently. The overall output effect of increasing or decreasing one of the variables may be the same independent of the other variable, but the magnitude is likely to vary. For an overview of the effect of changing channel thickness, Fig. 8 shows results for constant flow rate $\dot{V} = 0.02$ cm^3 s^{-1}. For that particular electrolyte flow rate, methanol crossover is kept low for all
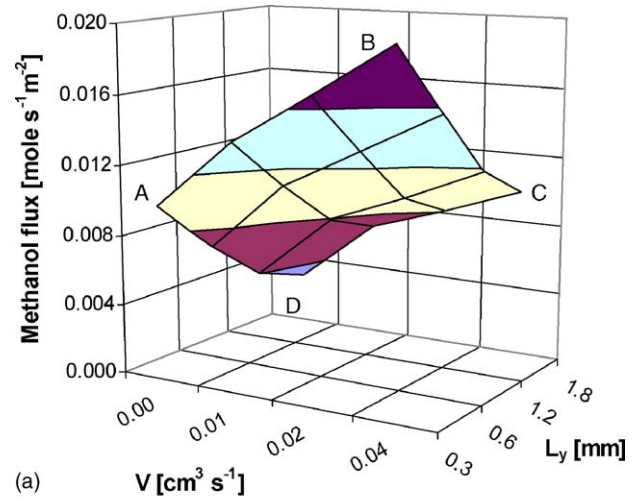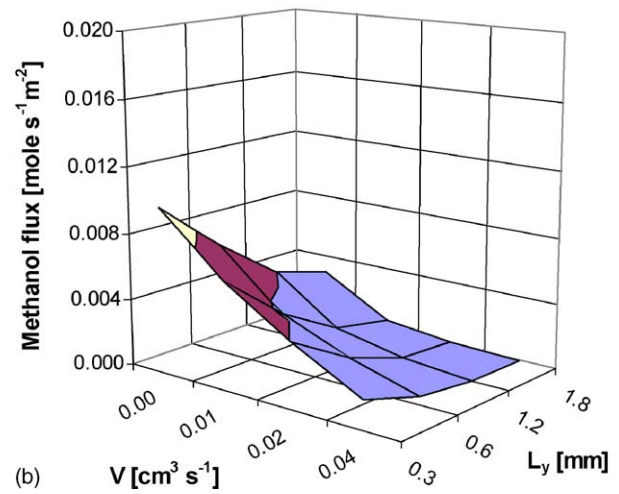
Fig. 6. Surface plots of average methanol molar flux density across (a) the anode surface (line AB and DC are at $L_y = 1.8$ mm, respectively); (b) the cathode surface (crossover), for different electrolyte flow rates and FE channel thickness. Anode fuel feed concentration is kept constant at 4 M.
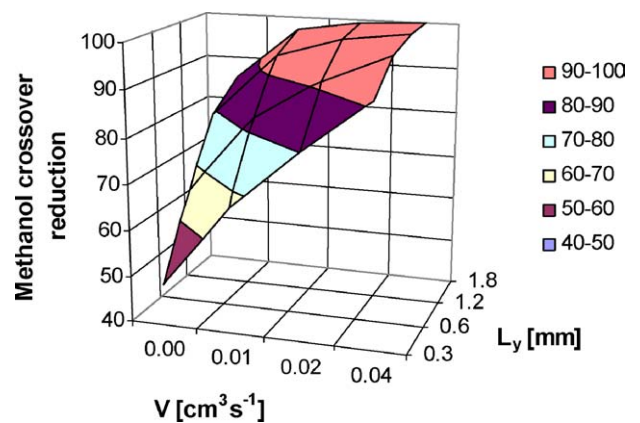

Fig. 7. Reduction of methanol crossover compared to the PEM-DMFC for various FE channel thicknesses and volumetric flow rates.
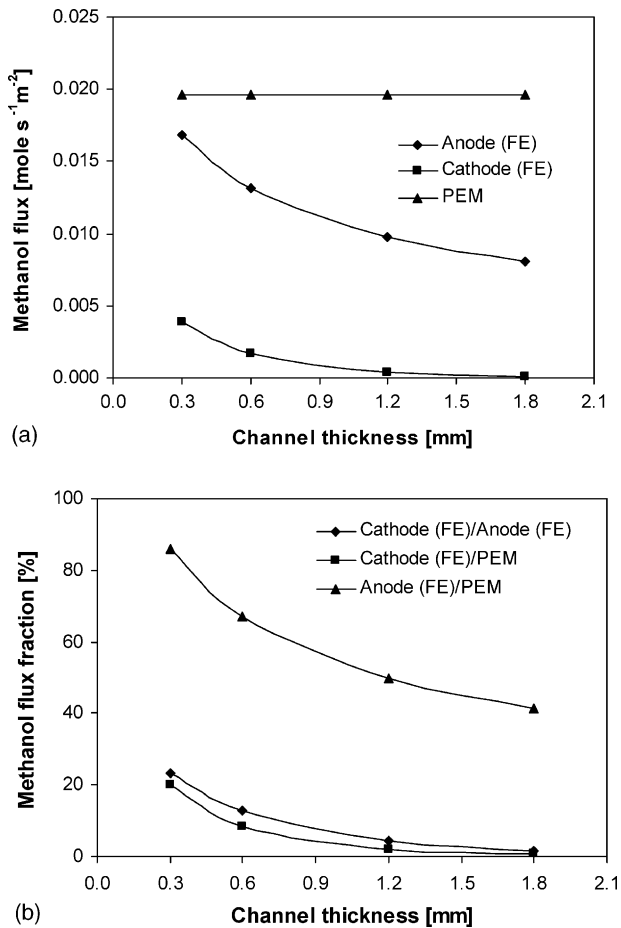
(a)

(b)

Fig. 8. (a) Average methanol molar flux density vs. FE channel thickness. (b) Molar flux density fractions. FE volumetric flow rate $0.02\,cm^3\,s^{-1}$ and anode surface concentration 4 M are kept constant.

channel thicknesses analyzed. For $L_y = 0.3$ mm, the crossover is reduced by 80% and for $L_y = 0.6$ mm the reduction is over 90% compared to the PEM-DMFC. The plots of Fig. 9 also take the other variable, electrolyte flow rate, into account. All four-channel thicknesses are analyzed and compared to the PEM case. The results once again indicate significant removal
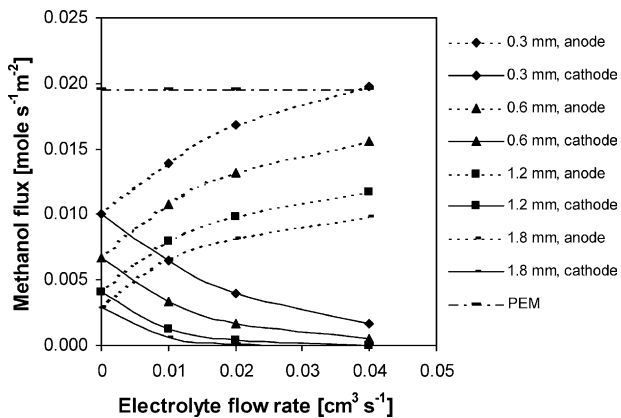

Fig. 9. Average methanol molar flux density vs. FE volumetric flow rate for different channel thickness. Anode surface concentration is constant at 4 M.
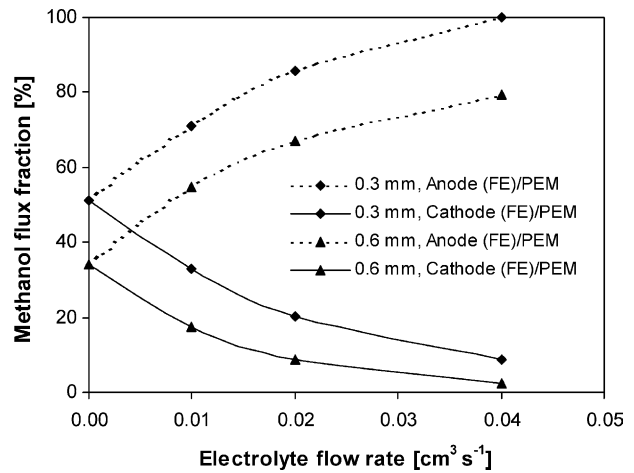

Fig. 10. Fractions of methanol molar flux at anode and cathode vs. electrolyte flow rate for channel thickness 0.3 and 0.6 mm. Anode surface concentration is 4 M.

of methanol by the flowing electrolyte. Methanol crossover is reduced, even with zero flow rates. However, there is a problem with the insertion of the electrolyte channel. There is always a certain resistance in the electrolyte, not only for methanol, but also for protons. To maintain a high cell voltage, the rate of proton transfer from anode to cathode must be kept high and steady. The Ohmic resistance is proportional to channel thickness, and it is important to avoid unnecessary thick channels. Thick channels also increase system size and weight. From this point of view, it is most likely better to increase the flow rate as a means of reducing crossover, and keep the channel thickness at a low value.

Fig. 10 displays fractions of methanol crossover for the 0.3 and 0.6 mm thick channels as a function of flow rate. For instance, if a crossover rate less than 20% (80% reduction) compared to the PEM-DMFC is desired, a 0.3 mm wide channel needs a flow rate of $0.02\,cm^3\,s^{-1}$ whereas for a 0.6 mm channel, $0.01\,cm^3\,s^{-1}$ is sufficient. For crossover rates below 10%, these flow rates should be doubled. The drawback with an increased electrolyte flow rate is the additional pump work needed. The pumping power must be monitored and included in an optimization study of the fuel cell performance.

To improve the performance of the FE-DMFC, the flowing electrolyte channel orientation is another important parameter. The function of the channel itself is not improved by changing its orientation, but its orientation art to the fuel channel is important. The anode surface concentration obviously depends on fuel channel orientation. Methanol concentration in the fuel feed has its maximum at the inlet and decreases gradually towards the outlet. Unlike the electrolyte channel, the fuel channel has several bends and a complex geometry. It extends over the anode surface like a maze. For the model, the fuel channel is assumed to be straight, with decreasing methanol concentration along the direction of the flow. This implies a linear anode surface concentration. There are three options of electrolyte and fuel channel orientations: parallel flow, counter flow and cross flow. Simulations of paral-
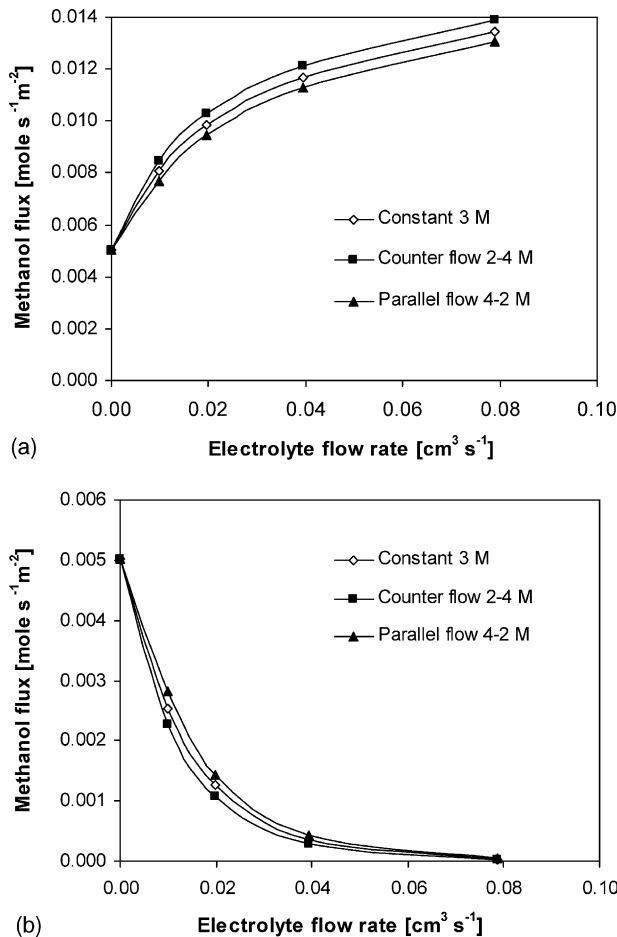
(a)

(b)

Fig. 11. Average anode (a) and cathode (b) methanol molar flux for the cases with constant anode concentration 3 M, parallel flow and counter flow with linear anode concentration from 4 to 2 M. Conditions: FE channel thickness 0.6 mm.
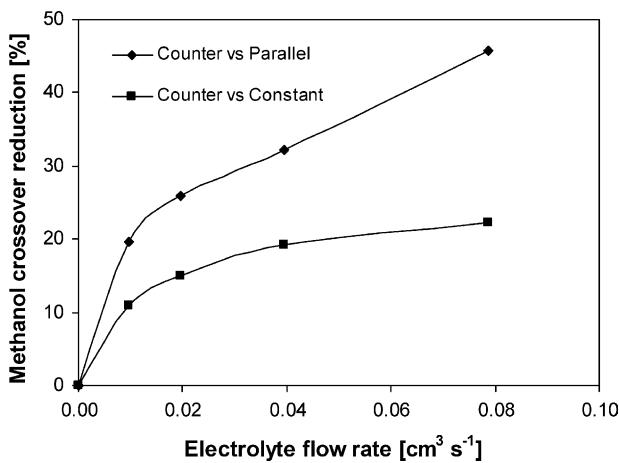

Fig. 12. Reduction of methanol crossover for counter flow compared to parallel flow and constant anode concentration. Conditions: FE channel thickness 0.6 mm.

lel flow and counter flow are performed for a linear anode concentration starting at 4 M and ending at 2 M. Simulation results are compared to the case of constant anode concentration $c_a = 3$ M in Fig. 11. Apparently, methanol crossover is lower for counter flow than for parallel flow although the anode flux is enhanced. For parallel flow, the crossover rate is even higher than for constant anode concentration. Fig. 12 presents an analysis of the accomplished crossover reduction for counter flow orientation. The results indicate excellent improvements using counter flow. For an electrolyte flow rate of 0.02 cm^3 s^{-1}, the reduction of methanol crossover is 26% and 15% compared to parallel flow and constant anode concentration, respectively.

5. Conclusions

A general three-dimensional numerical CFD model of the flowing electrolyte-direct methanol fuel cell is used to simulate methanol crossover by convection and diffusion for a variety of operating conditions. Methanol concentration distribution and methanol molar flux densities are presented for the full geometry of the MEA. Compared to the equivalent proton exchange membrane direct methanol fuel cell, methanol crossover is greatly reduced due to enhanced mass transfer by convection (90% reduction for reference operating conditions). The rate of crossover is shown to be higher in the presence of concentration edge effects near the outer edges of the electrolyte channel than in the bulk of the electrolyte flow. It is also more severe near the outlet than at the inlet part of the channel.

For a thorough study of various parameters and operating conditions, the general model has to be simplified based on a slice in the middle of the electrolyte channel, which ignores the edge effects. This study focuses on the effect of anode surface methanol concentration, flowing electrolyte channel thickness and volumetric flow rate. The average methanol molar flux density across the cathode surface (average methanol crossover) is shown to be directly proportional to the anode surface concentration. Combined analyses confirm that methanol crossover is inversely proportional to both channel thickness and flow rate. Thus, wide channels and high flow rates are needed to minimize it. Due to the amplified Ohmic resistance arising for wide channels, it might be a better strategy to increase the flow rate than the channel thickness. But with increased flow rate, it is important to monitor the pump work needed and make sure it does not substantially reduce the system efficiency.

The convection mechanism also affects methanol flux across the anode surface. High flow rates and low channel thicknesses lead to enhanced anode methanol suction. This improves mass transfer in the anode catalyst layer, which may also improve the reaction rate. However, more fuel will be mixed in the electrolyte, which calls for external processing to maintain fuel efficiency. The anode flux is nevertheless significantly lower than for the PEM-DMFC.

For the case of linearly decreasing anode fuel concentration from inlet to outlet of the fuel channel, different electrolyte channel orientations are considered. Parallel flow and counter flow are both compared to the general case of constant anode concentration. To reduce fuel crossover, counter flow is shown to be the superior channel orientation.

The model can be improved further by adding the contributions of electro-osmosis and pressure gradients to the rate of methanol crossover, which is an ongoing work. More accurate values of the diffusivity of methanol in Nafion$^®$ and water also need to be determined. Further work includes modeling polarization characteristics and determining the Ohmic resistance of the electrolyte. The overall objective is to optimize the flowing electrolyte channel by comparing gain in voltage by reduction of methanol crossover to Ohmic losses and electrolyte pump work. Additional experiments and measurements of methanol crossover in the FE-DMFC would also be desired.

References

[1] P. Ahlvik, Å. Brandberg, Well-To Wheel Efficiency for Alternative Fuels from Natural Gas or Biomass, Publication number 2001:85, Swedish National Road Administration, Borlänge, Sweden, 2001.

[2] J. Larminie, A. Dicks, Fuel Cell Systems Explained, second ed., John Wiley & Sons Ltd., Chichester, UK, 2003.

[3] A. Heinzel, V.M. Barragan, A review of the state-of-the-art of the methanol crossover in direct methanol fuel cells, J. Power Sources 84 (1999) 70–74.

[4] B. Smitha, S. Sridhar, A.A. Khan, Polyelectrolyte complexes of chitosan and poly (acrylic acid) as proton exchange membranes for fuel cells, Macromolecules 37 (2004) 2233–2239.

[5] E. Peled, T. Duvdevani, A. Aharon, A. Melman, A direct methanol fuel cell based on a novel low-cost nanoporous proton-conducting membrane, Electrochem. Solid-State Lett. 3 (12) (2000) 525–528.

[6] J. Liu, H. Wang, S. Cheng, K.Y. Chan, Nafion-polyfurfuryl alcohol nanocomposite membranes with low methanol permeation, Chem. Commun. (2004) 728–729.

[7] M.K. Song, S.B. Park, Y.T. Kim, H.W. Rhee, J. Kim, Nanocomposite polymer membrane based on cation exchange polymer and nano-dispersed clay sheets, Mol. Cryst. Liq. Cryst. 407 (2003) 411–419.

[8] J.H. Shim, S.M. Song, W.K. Her, I.G. Koo, W.M. Lee, Electrochemical acceleration of hydrogen transfer through a methanol impermeable metallic barrier, J. Electrochem. Soc. 150 (12) (2003) A1583–A1588.

[9] K. Kordesch, M. Cifrain, T. Hejze, V. Hacker, U. Bachhiesl, Fuel circulating electrolytes, in: Proceedings of the Fuel Cell Seminar 2000, Portland, 30 October–2 November, 2000, pp. 432–435.

[10] K. Kordesch, V. Hacker, U. Bachhiesl, Direct methanol-air fuel cells with membranes plus circulating electrolyte, J. Power Sources 96 (2001) 200–203.

[11] K. Sundmacher, T. Schultz, S. Zhou, K. Scott, M. Ginkel, E.D. Gilles, Dynamics of the direct methanol fuel cell (DMFC): experiments and model-based analysis, Chem. Eng. Sci. 56 (2001) 333–341.

[12] Z.H. Wang, C.Y. Wang, Mathematical modeling of liquid-feed direct methanol fuel cells, J. Electrochem. Soc. 150 (4) (2003) A508–A519.

[13] M.R. Golriz, J. Gu, D. James, Mass transport inside a flowing electrolyte-direct methanol fuel cell, in: R.K. Shah, S.G. Kandlikar (Eds.), Fuel Cell Science, Engineering and Technology, ASME, NY, 2004, pp. 107–112.

[14] H. Guo, C.F. Ma, 2D analytical model of a direct methanol fuel cell, Electrochem. Commun. 6 (3) (2004) 306–312.

[15] J. Cruickshank, K. Scott, The degree and effect of methanol crossover in the direct methanol fuel cell, J. Power Sources 70 (1998) 40–47.

[16] K. Scott, W. Taama, J. Cruickshank, Performance of a direct methanol fuel cell, J. Appl. Electrochem. 28 (1998) 289–297.

[17] A.A. Kulikovsky, Two-dimensional numerical modeling of a direct methanol fuel cell, J. Appl. Electrochem. 30 (2000) 1005–1014.

[18] C. Nordling, J. Österman, Physics Handbook, sixth ed., Studentlitteratur, Lund, Sweden, 1999.